J|A|C|S
ARTICLES
Published on Web 05/30/2002

Structural Chemistry of *arachno*-Nonaboranes

Jonathan Bould,[†,‡,§] Robert Greatrex,[†] John D. Kennedy,[†] Daniel L. Ormsby,[†] Michael G. S. Londesborough,[†] Karen L. F. Callaghan,[†] Mark Thornton-Pett,[†] Trevor R. Spalding,[§] Simon J. Teat,[||] William Clegg,[⊥] Hong Fang,[‡] Nigam P. Rath,[‡] and Lawrence Barton*[,‡]

Contribution from the School of Chemistry, University of Leeds, Leeds, U.K. LS2 9JT, Department of Chemistry, University of Missouri—St. Louis, St. Louis, Missouri 63121, Department of Chemistry, University College Cork, Cork, Ireland, CCLRC Daresbury Laboratory, Daresbury, Warrington, U.K. WA4 4AD, and Department of Chemistry of the University of Newcastle, Newcastle upon Tyne, U.K. NE1 7RU

Received January 24, 2002

Abstract: Single-crystal conventional-tube and synchrotron X-ray diffraction studies of the anions in [NMe_4][*arachno*-B_9H_{12}-4,8-Br_2] **1** and K[*arachno*-B_9H_{14}] **2**, and also of the series of adducts [*arachno*-B_9H_{13}-4-L], where L is $P(CCH)_3$ (**3**), $NHEt_2$ (**4**), NC_5H_5 (**5**), or NH_2CH_2Ph (**6**), are reported. Structural studies of **1**−**6**, determined at low temperatures, located all atoms, including bridging and *endo*-terminal hydrogen atoms. The basic boron-hydride clusters of these, and of all the other known species with the *arachno* nine-vertex *i*-nonanborane geometry reported in the literature, are isostructural and feature three bridging and two *endo*-terminal hydrogen atoms on the open face. This arrangement is different from that previously reported for Cs[*arachno*-B_9H_{14}] **7** and for [*arachno*-B_9H_{13}-4-(NCMe)] **9**. However, a new X-ray diffraction data set and refinement experimentally confirm the {3 × μ-H, 2×*endo*} arrangement for **9** also. The experimental results for **1**−**6** support recently reported calculations for $[B_9H_{14}]^-$, which predict both the structures and the ^{11}B NMR chemical shifts. These conclusions are also supported by calculations for **3**, **4**, and **9** and also for the [*arachno*-B_9H_{13}-4-(NCS)]$^-$ anion in [NMe_4][B_9H_{13}(NCS)] **8**.

Introduction

The *arachno* nine-boron nine-vertex borane clusters dealt with in this paper constitute a fundamental boron-hydride cluster type. Their *i*-nonaborane structures provide an interesting and consistent deviation from the coordination number pattern recognition theory for boranes and carboranes, as described by Williams in 1971.[1] This theory requires that, to generate *arachno* clusters from *nido* systems, a highest connectivity vertex, adjacent to the open face, is removed. Thus, starting from the geometry of *nido*-$B_{10}H_{14}$, the *arachno* nine-vertex configuration **I** (Chart 1) would be generated. However, this configuration, known by historical precedent as the normal or *n* geometry,[2] is in fact rare, being exhibited in binary boranes only by *n*-B_9H_{15} itself[2] and by isolated examples of metallaboranes such as [η^6-(C_6Me_6)RuB_8H_{14}][3a] and [{(dppe)Pt}$_2B_7H_{11}$],[3b] and more occasionally by metallaheteroboranes such as [$(PMe_2Ph)_2PtB_7H_{10}$-NHEt].[3c] An alternative configuration **II**, also shown in Chart 1, is derived by the removal of a vertex of low connectivity from *nido*-$B_{10}H_{14}$ (structure **III** in Chart 1). This geometry, discovered after the species of *n* geometry and therefore given an *iso* or *i* descriptor, is in fact much more prevalent, being exhibited by the parent cluster *i*-B_9H_{15}[2] and by the $[B_9H_{14}]^-$ anion[4] and by a series of neutral ligand derivatives [B_9H_{13}L],[5] in addition to being ubiquitous as the fundamental structural motif for whole families of heteroborane derivatives[6] based on $[CB_8H_{14}]$,[6,7] $[NB_8H_{13}]$,[8a] $[SB_8H_{12}]$,[6,8c,9] $[C_2B_7H_{13}]$,[10] $[S_2B_7H_9]$,[8b,11] etc., as well as metallaborane families represented by [(CO)-

Chart 1

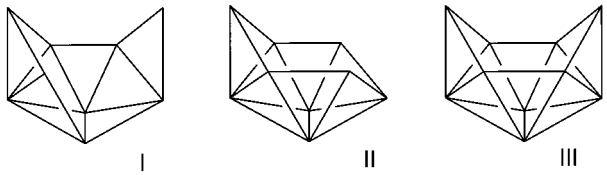

* Corresponding author: e-mail lbarton@jinx.umsl.edu; fax 314-516-5342.
[†] University of Leeds.
[‡] University of Missouri—St. Louis.
[§] University College Cork.
[||] CCLRC Daresbury Laboratory.
[⊥] University of Newcastle.

(1) Williams, R. E. *Inorg. Chem.* **1971**, *1*, 210; *Adv. Inorg. Chem. Radiochem.* **1976**, *18*, 64.
(2) Barton, L. *Top. Curr. Chem.* **1982**, *100*, 169.
(3) (a) Bown, M.; Fontaine, X. L. R.; Greenwood, N. N.; Kennedy, J. D.; Thornton-Pett, M. *J. Organomet. Chem.* **1986**, *315*, C1. (b) Macías, R.; Rath, N. P.; Barton, L. *J. Chem. Soc., Chem. Commun.* **1998**, 1081. (c) Dörfler, U.; Salter, P. A.; Fontaine, X. L. R.; Greenwood, N. N.; Kennedy, J. D.; Thornton-Pett, M. *Collect. Czech. Chem. Commun.* **1999**, *64*, 947.
(4) Barton, L.; Onak, T. P.; Shore, S. G. *Gmelin Handbook of Inorganic Chemistry*, *Boron Compounds 20*; New Supplement Series, Vol. 54; Springer-Verlag: Berlin, 1979; pp 113−118.
(5) See, for example, together with references therein: Shore, S. G. In *Boron Hydride Chemistry*; Muetterties, E. L., Ed.; Academic Press: New York, 1975; pp 79−174.
(6) Holub, J.; Jelínek, T.; Štíbr, B.; Kennedy, J. D.; Thornton-Pett, M. In *Current Topics in the Chemistry of Boron*; Kabalka, G. W., Ed.; The Royal Society of Chemistry: Cambridge, U.K., 1994; pp 359−362.

$(PMe_3)_2HIrB_8H_{12}]$[12] and $[(PMe_2Ph)_2PtB_8H_{12}]$[13] and isolated metallaheteroboranes such as $[(PPh_3)_2PtCB_7H_{11}]$[14a] and $[(PMe_2Ph)_2PtS_2B_6H_8]$.[14b] However, despite the ubiquity of this structural motif **II**, there are inconsistencies, both within the literature and between literature reports and our own experimental findings, concerning the fundamental hydrogen-atom configurations in its basic nine-boron templates $[B_9H_{14}]^-$ and $[B_9H_{13}L]$. We now address these inconsistencies and attempt to resolve them in this present paper.

Discussion of Background

The initial structural studies on the *i*-nonaborane class of *arachno* compounds were conducted many years ago.[15,16] Thus, the [*arachno*-$B_9H_{13}L$] compound **9**, where L is the Lewis-base two-electron donor ligand MeCN, was structurally characterized by Lipscomb and co-workers in 1961,[15b,c] following the original synthesis by Hawthorne and co-workers in 1960.[15a] The existence of the related $[B_9H_{14}]^-$ anion was predicted by Lipscomb in 1961[15b] and structurally characterized by Greenwood and co-workers in its Cs^+ salt, compound **7**, in 1970.[16b,c] It was originally synthesized by Takacs and co-workers in 1963.[16a] Because of the nature of the results, discussion and conclusions in this present paper below, some detail of this background is required.

Chart 2

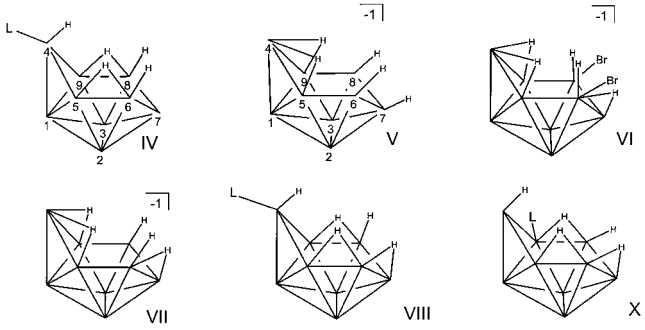

The diffraction analysis of compound **9** indicated a nine-vertex polyhedron as in structure **II**, with two bridging and three *endo*-terminal hydrogen atoms in addition to nine *exo*-terminal hydrogen atoms and an *exo*-terminal ligand in the 4-position, giving the [*arachno*-B_9H_{13}-4-L] formulation represented in Chart 2, structure **IV**. [Note that in the structures in the present paper, the vertexes are BH(*exo*) units and all the *endo*- and bridging hydrogen atoms are shown; in structures **VI** and **XI**, the non-hydrogen *exo*-substituents, Br in **VI** and L in **X**, are included.] The configuration of **IV** would not be inconsistent with the solution ^{11}B and ^1H NMR data, which exhibit the expected respective 2:2:2:1:1:1 and 2:2:2:2:1:1:1:2 relative-intensity patterns for a species with C_s symmetry.[17] Somewhat later, results from the structural investigation of the isoelectronic, and formally isostructural, [*arachno*-$B_9H_{14}]^-$ anionic species in its Cs^+ salt **7**, by an ambient-temperature X-ray diffraction analysis allied with NMR spectroscopic methods, were interpreted in terms of a very similar basic $\{2\times\mu H, 3\times endo\}$ structure.[16b,c] This derived structure differed from that of the $[B_9H_{13}(NCMe)]$ species in the relative positioning of its open-face inner-sphere[18] $\{2\times\mu H, 3\times endo\}$ hydrogen atom configuration but was otherwise analogous. Specifically, it had two adjacent bridging hydrogen atoms at a $\{BH(\mu\text{-}H)_2\}$ vertex and three mutually adjacent *endo*-terminal hydrogen atoms, as in structure **V**. In contrast to the neutral $[B_9H_{13}L]$ species, the relative-intensity patterns in the ^{11}B and ^1H solution NMR spectra of $[B_9H_{14}]^-$ are not consistent with the derived solid-state structure. Instead the ^{11}B spectrum has a 3:3:3 relative intensity pattern whereas the ^1H spectrum has a 3:3:3:5 pattern. These simpler patterns arise from a fluxionality in solution among all five open-face inner-sphere hydrogen atoms, as discussed further below. These two hydrogen-atom configurations, viz., **V** for the [*arachno*-$B_9H_{14}]^-$ anion and **IV** for the neutral ligand species [*arachno*-B_9H_{13}-4-L], have hitherto been generally regarded as defining these two basic types.

More recently, and reported contemporaneously with the definitive experimental work reported herein, ab initio/IGLO/NMR studies of the [*arachno*-$B_9H_{14}]^-$ anion and of neutral [*arachno*-B_9H_{13}-4-(NCMe)] have been conducted by Hofmann and Schleyer.[19] Their results indicate that the ground state for the $[B_9H_{14}]^-$ anion should feature three bridging and two *endo*-terminal hydrogen atoms about the open face of the cluster as

(7) Holub, J.; Jelínek, T.; Plesek, J.; Štíbr, B.; Heřmánek, S.; Kennedy, J. D. *J. Chem. Soc., Chem. Commun.* **1991**, 1389. (b) Štíbr, B. *Chem. Rev.* **1992**, *92*, 245.
(8) (a) Baše, K.; Plešek, J.; Heřmánek, S.; Huffman, J.; Ragatz, P.; Schaeffer, R. *J. Chem. Soc., Chem. Commun.* **1975**, 934. (b) Baše, K.; Hanousek, F.; Plešek, J.; Štíbr, B.; Lyčka, A. *J. Chem. Soc., Chem. Commun.* **1981**, 1162. (c) Baše, K. *Collect. Czech. Chem. Commun.* **1983**, *48*, 2593. (d) Štíbr, B.; Kennedy, J. D.; Jelínek, T. *J. Chem. Soc., Chem. Commun.* **1990**, 1309. (d) Jelínek, T.; Štíbr, B.; Kennedy, J. D. *Collect. Czech. Chem. Commun.* **1994**, *59*, 2244. (e) Roth, M.; Paetzold, P. *Chem. Ber.* **1995**, *126*, 1221. (e) Price, C.; Dörfler, U.; Kennedy, J. D.; Thornton-Pett, M. *Acta Crystallogr, Sect. C* **2000**, *56*, 600.
(9) (a) Pretzer, W. R.; Rudolph, R. W. *J. Am. Chem. Soc.* **1976**, *98*, 1441. (b) Base, K.; Gregor, V.; Heřmánek, S. *Chem. Ind. (London)* **1979**, 743. (c) Baše, K.; Štíbr, B.; Zakharova, I. A. *Synth. React. Inorg. Metal-Org. Chem.* **1980**, *10*, 509. (d) Kang, S. O.; Sneddon, L. G. *Inorg. Chem.* **1988**, *27*, 3298. (e) Baše, K.; Wallbridge, M. G. H.; Fontaine, X. L. R.; Greenwood, N. N.; Jones, J. H.; Kennedy, J. D.; Štíbr, B. *Polyhedron*, **1989**, *8*, 2089. (f) Holub, J.; Kennedy, J. D.; Štíbr, B. *Collect. Czech. Chem. Commun.* **1994**, *59*, 367.
(10) (a) Rietz, R. R.; Schaeffer, R. *J. Am. Chem. Soc.* **1971**, *93*, 1263, and **1973**, *95*, 6254. (b) Plešek, J.; Štíbr, B.; Heřmánek, S. *Chem. Ind. (London)* **1980**, 626. (c) Štíbr, B.; Plešek, J.; Heřmánek, S. *Inorg. Synth.* **1983**, *22*, 237. (d) Heřmánek, S.; Jelínek, T.; Plešek, J.; Štíbr, B.; Fusek, J. *J. Chem. Soc., Chem. Commun.* **1987**, 927; *Collect. Czech. Chem. Commun.* **1988**, *53*, 2742. (e) Jelínek, T.; Holub, J.; Štíbr, B.; Fontaine, X. L. R.; Kennedy, J. D. *Collect. Czech. Chem. Commun.* **1994**, *59*, 1584.
(11) (a) Plešek, J.; Heřmánek, S.; Janoušek, Z. *Collect. Czech. Chem. Commun.* **1977**, *42*, 785. (b) Jones, J. H.; Fontaine, X. L. R.; Greenwood, N. N.; Kennedy, J. D.; Thornton-Pett, M.; Štíbr, B.; Langhoff, H. *J. Organomet. Chem.* **1993**, *445*, C15.
(12) (a) Bould, J.; Crook, J. E.; Greenwood, N. N.; Kennedy, J. D. *J. Chem. Soc., Dalton Trans.*, **1984**, 1903. (b) Bould, J.; Rath, N. P.; Barton, L. *Organometallics* **1996**, *15*, 4916. (c) Bould, J.; Rath, N. P.; Barton, L.; Kennedy, J. D. *Organometallics* **1998**, *17*, 902. (d) Bould, J.; Kennedy, J. D.; Thornton-Pett, M.; Barton, L.; Rath, N. P. *Acta Crystallogr., Sect. C* **2001**, *57*, 49.
(13) (a) Boocock, S. K.; Greenwood, N. N.; Hails, M. J.; Kennedy, J. D.; McDonald, W. S. *J. Chem. Soc., Dalton Trans.* **1981**, 1415−1429. (b) Bould, J.; Clegg, W.; Teat, S. J.; Barton, L.; Rath, N. P.; Thornton-Pett, M.; Kennedy, J. D. *Inorg. Chim. Acta* **1999**, *289*, 95−124.
(14) (a) Jones, J. H.; Štíbr, B.; Kennedy, J. D.; Lawrence, A. D.; Thornton-Pett, M. *J. Chem. Soc., Dalton Trans.* **1993**, 1269. (b) Ferguson, G.; McCarthy, D. E.; Spalding T. R.; Kennedy, J. D. *Acta Crystallogr., Sect. C* **1996**, *52*, 548.
(15) (a) Hawthorne, M. F.; Graybill, B. M.; Pitochelli, A. R. *Abstracts of the 138th National Meeting of the American Chemical Society*, Paper 45N; September 11−16, 1960, New York. (b) Wang, F. E.; Simpson, P. G.; Lipscomb, W. N. *J. Am. Chem. Soc.* **1961**, *83*, 491. (c) Wang, F. E.; Simpson, P. G.; Lipscomb, W. N. *J. Chem. Phys.* **1961**, *35*, 1335.
(16) (a) Benjamin, L. E.; Stafiej, S. F.; Takacs, E. A. *J. Am. Chem. Soc.* **1963**, *85*, 2674. (b) Greenwood, N. N.; Gysling, H. J.; McGinnety, J. A.; Owen, J. D. *J. Chem. Soc., Chem. Commun.* **1970**, 505. (c) Greenwood, N. N.; Gysling, H. J.; McGinnety, J. A.; Owen, J. D. *J. Chem. Soc., Dalton Trans.* **1972**, 986.
(17) Jacobsen, G. B.; Meina, D. G.; Morris, J. H.; Thompson, C.; Andrews, S. J.; Reed, D.; Welch, A. J.; Gaines, D. F. *J. Chem. Soc., Dalton Trans.* **1985**, 1645.
(18) Inner sphere refers to *endo*- and bridging-H atoms in single polyhedral borane fragments, as defined by Lipscomb, W. N. *Boron Hydrides*; W. A. Benjamin: New York, 1963; p 53.
(19) Hofmann, M.; Schleyer, P. v. R. *Inorg. Chem.* **1999**, *38*, 652.

in structure **VII**, in contrast to the {2×μ-H, 3×*endo*} arrangement **V** suggested from the earlier X-ray diffraction analysis by Greenwood et al.[16b,c] The calculational results similarly indicate that the cluster of neutral $[B_9H_{13}(NCMe)]$ should also possess the {3×μ-H, 2×*endo*} arrangement of its inner-sphere hydrogen atoms (structure **VIII**), in contrast to the previously supposed[15b,c] {2×μ-H, 3×*endo*} arrangement **IV**.

Since the publication of the experimentally determined structures of these two compounds there have been only two further structural characterizations of the *arachno*-B_9 species described in the literature, viz., the [*arachno*-$B_9H_{13}(NCS)]^-$ anion,[20] where the ligand is the formally anionic pseudohalide $[SCN]^-$, and a more recent report for the neutral compound [*arachno*-B_9H_{13}-5-(NC_5H_4-4-Ph)] (structure **X**), a structural isomer of the [*arachno*-B_9H_{13}-4-L] species discussed above.[21] Both these species show the {3×μ-H, 2×*endo*} arrangement of hydrogen atoms, rather than the {2×μ-H, 3×*endo*} configuration originally deduced for $[B_9H_{13}(CNMe)]$. Several other $[B_9H_{13}L]$ species have also been known for some time,[5,22] but their structures also have generally been presumed to have the {2×μ-H, 3×*endo*} configuration **IV** on the basis of NMR spectroscopy and the original $[B_9H_{13}(CNMe)]$ structural result. For completeness here, it should also be noted that a nonjournal structural report by Huffman on the $[B_9H_{14}]^-$ anion can be invoked.[23] In this, the X-ray analysis, on diffraction data gathered at low temperature, also indicated the {3×μ-H, 2×*endo*} configuration **VII** rather than the {2×μ-H, 3×*endo*} configuration **V**.

Elements of our own entry into this area arose during the search for new routes to large macropolyhedral borane, heteroborane, and metallaborane cluster compounds.[24] For these studies, we attempted to synthesize quantities of the octadecaborane compound *anti*-$B_{18}H_{22}$[17,25] by the method of Gaines et al.[26] This procedure forms *anti*-$B_{18}H_{22}$ in a reported yield of ca. 40% via the reaction of the [*nido*-$B_9H_{12}]^-$ anion with $HgBr_2$ in CH_2Cl_2 solution. In our hands, however, we have so far been able to realize yields of *anti*-$B_{18}H_{22}$ of only ca. 20%, with the main products appearing to be halogenated nonaborane species, in inconsistent yields of up to 36%. Although the presence of these compounds was noted by the original authors, they were unable to characterize them satisfactorily.[27] We therefore carried out low-temperature single-crystal X-ray diffraction and NMR spectroscopic studies on the major halogenated nonaborane byproduct, which is thereby identified as the [*arachno*-B_9H_{12}-4,8-$Br_2]^-$ anion, isolated as its $[NMe_4]^+$ salt (compound **1**). Interestingly, our analysis of this compound showed significant differences in the arrangement of hydrogen atoms on the open face of the cluster (see also structure **II**), compared to the arrangement **V** concluded from the original ambient-temperature study of the unsubstituted but otherwise equivalent [*arachno*-$B_9H_{14}]^-$ anion in its Cs^+ salt **7**.[16b,c] In view of this, therefore, and in view also of Huffman's conflicting analysis of the Cs^+ salt **7** to give arrangement **VII**,[23] we have undertaken also the low-temperature structural study of this $[B_9H_{14}]^-$ anion as its K^+ salt (compound **2**),[28] in order to clarify its open-face hydrogen-atom distribution. This last study shows a parallel with the {3×μ-H, 2×*endo*} arrangement **VI** of open-face hydrogen atoms determined for the dibromo compound **1** rather than with the {2×μ-H, 3×*endo*} arrangement **V** reported by Greenwood et al.[16b,c] for the Cs^+ compound **7**. The {3×μ-H, 2×*endo*} arrangement **VII** is consistent with the calculations of Hofmann and Schleyer mentioned above[19] and is also in accord with that described in the 19-year-old nonjournal report of a low-temperature X-ray diffraction study of the Cs^+ salt of $[B_9H_{14}]^-$ (compound **7**) also mentioned above.[23]

The other set of *arachno* nonaboranes of configuration **II** are the ligand derivatives [*arachno*-B_9H_{13}-4-L], and as mentioned above, there is a related inconsistency in the literature regarding the hydrogen-atom distribution for this set of compounds also. To address this inconsistency, we also report here the structures and NMR spectra for the mutually related isoelectronic and isostructural series of *arachno*-nonaborane adducts [B_9H_{13}-4-L], where L is $P(CCH)_3$ (**3**), $NHEt_2$ (**4**), NC_5H_5 (**5**), or NH_2CH_2Ph (**6**). These last four species, compounds **3**−**6**, were isolated from a number of unrelated parallel studies but it is appropriate to report them together herein. They all exhibited the {3×μ-H, 2×*endo*} configuration **VIII**, consistent with the results obtained for the $[B_9H_{13}(NCS)]^-$ anion[20] and consistent with the calculations of Hofmann and Schleyer.[19] However, they do not concur with the {2×μ-H, 3×*endo*} configuration **IV** originally reported[15b,c] for neutral $[B_9H_{13}(NCMe)]$ **9**. We therefore undertook a collection and analysis of single-crystal X-ray diffraction data for **9** at low temperature. This enabled a reassessment, and a new refinement, which now indicates the {3×μ-H, 2×*endo*} structure **VIII** for this last species also. The dichotomy between the observed 2:2:2:1:1:1 ^{11}B NMR relative intensity pattern and the pattern of nine signals of equal intensity expected for configuration **VIII** arises because of fluxional exchange in solution between *endo* and bridging positions for the two inner-sphere open-face hydrogen atoms associated with the B6B7B8 site,[19] as discussed in more detail below. Here it

(20) Andrews, S. J.; Welch, A. J. *Acta Crystallogr.* **1985**, *C41*, 1208.
(21) Callaghan, K. L. F.; Dörfler, U.; McGrath, T. D.; Thornton-Pett, M.; Kennedy, J. D. *J. Organomet. Chem.* **1998**, *550*, 441.
(22) (a) Bodner, G. M.; Scholer, F. R.; Todd, L. J.; Senor, L. E.; Carter, J. C. *Inorg. Chem.* **1971**, *10*, 942.(b) Hermánek, S.; Plešek, J.; Štíbr, B.; Hanoušek, F. *Collect. Czech. Chem. Commun.* **1968**, *33*, 2177. (c) Schaeffer, R.; Walter, E. *Inorg. Chem.* **1973**, *12*, 2209. (d) Jacobsen, G. B.; Morris, J. H.; Reed, D. *J. Chem. Soc., Dalton Trans.* **1984**, 415. (e) Naoufal, D.; Grüner, B.; Bonnetot, B.; Mongeot, H. *Main Group Met. Chem.* **1999**, *22*, 127.
(23) Huffman, J. D. Report 82210, Molecular Structure Center, Indiana University Department of Chemistry, 1982. Cited in Getman, T. D.; Krause, J. A.; Niedenzu, P. M.; Shore, S. G. *Inorg. Chem.* **1989**, *28*, 1507.
(24) (a) Bould, J.; Greenwood, N. N.; Kennedy, J. D. *Polyhedron*, **1983**, *2*, 1401. (b) Kaur, P.; Holub, J.; Rath, N. P.; Bould, J.; Barton, L.; Štíbr, B.; Kennedy, J. D. *J. Chem. Soc., Chem. Commun.* **1996**, 273. (c) Barton, L.; Bould, J.; Kennedy, J. D.; Rath, N. P. *J. Chem. Soc., Dalton Trans.* **1996**, 3145. (d) Bould, J.; Clegg, W.; Kennedy, J. D.; Teat, S. J.; Thornton-Pett, M. *J. Chem. Soc., Dalton Trans.* **1997**, 2005. (e) Bould, J.; Kennedy, J. D.; Barton, L.; Rath, N. P. *J. Chem. Soc., Chem. Commun.* **1997**, 2405. (f) Bould, J.; Clegg, W.; Kennedy, J. D.; Teat, S. J. *J. Chem. Soc., Dalton Trans.* **1998**, 2777. (g) Bould, J.; Barrett, S. A.; Barton, L.; Rath, N. P.; Kennedy, J. D. *Inorg. Chem. Commun.* **1998**, *1*, 365. (h) Bould, J.; Clegg, W.; Teat, S. J.; Barton, L.; Rath, N. P.; Thornton-Pett, M.; Kennedy, J. D. *Inorg. Chim. Acta* **1999**, *289*, 95.
(25) (a) Pitochelli, A. R.; Hawthorne, M. F. *J. Am. Chem. Soc.* **1962**, *84*, 3218. (b) Olsen, F. P.; Vasavada, R. C.; Hawthorne, M. F. *J. Am. Chem. Soc.* **1968**, *90*, 3941. (c) Plešek, J.; Heřmánek, S.; Štíbr, B.; Hanousek, F. *Collect. Czech. Chem. Commun.* **1967**, *32*, 1095. (d) Plešek, J.; Heřmánek, S.; Hanousek, F. *Collect. Czech. Chem. Commun.* **1968**, *33*, 699. (e) Dobson, J.; Keller, P. C.; Schaeffer, R. *Inorg. Chem.* **1968**, *7*, 399. (f) McAvoy, J. S.; Wallbridge, M. G. H. *J. Chem. Soc., Chem. Commun.* **1969**, 1378. (g) Bould, J.; Greenwood, N. N.; Kennedy, J. D. *Polyhedron* **1983**, *2*, 1401. (h) Kang, S. O.; Sneddon, L. G. *Inorg. Chem.* **1988**, *27*, 587. (i) Lawrence, S. H.; Wermer, J. R.; Boocock, S. K.; Banks, M. A.; Keller, P. C.; Shore, S. G. *Inorg. Chem.* **1986**, *25*, 367.
(26) Gaines, D. F.; Nelson, C. K.; Steehler, G. A. *J. Am. Chem. Soc.* **1984**, *106*, 7266.
(27) Gaines, D. F. Personal communication to J. B. at BUSA-V-MEX, Guanajuato, Mexico, 1996.
(28) Fang, H. Ph.D. dissertation, University of Missouri, St. Louis, 1996 [*Diss. Abstr. Intl.* **1995**, *56*, B 4306].

Chart 3

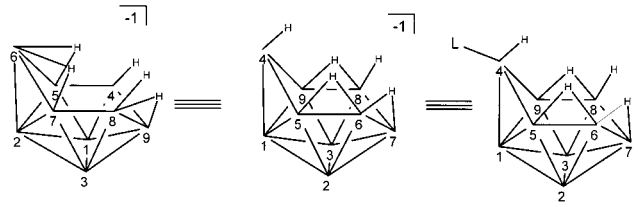

is convenient to note that numbering schemes for the anionic and ligated compounds have differed historically due to their perceived structural differences. However, as we describe below, the clusters of both classes can now be regarded as isostructural in terms of their {3×μ-H, 2×*endo*} hydrogen-atom distribution. We have, therefore, adopted a single numbering scheme that is based on the [*arachno*-B_9H_{13}-4-L] compounds as shown in Chart 3.

Experimental Section

The compounds [NMe_4][*nido*-B_9H_{12}][29] and triethynylphosphine, [$P(CCH)_3$],[30] were prepared according to literature methods, and $HgBr_2$ was used as received (Aldrich). The samples of [*arachno*-B_9H_{13}-4-($NHEt_2$)] **4**, [*arachno*-B_9H_{13}-4-(SMe_2)], and [*arachno*-B_9H_{13}-4-(NCMe)] **9** were prepared by literature methods.[31,22] The sample of K[*arachno*-B_9H_{14}] **2** was obtained serendipidously in attempts to obtain single crystals from solutions of [$Cd(B_5H_8)_2$] in tetrahydrofuran that also contained KCl.[28] Solvents were dried by standard methods, and reactions were carried out under dry dinitrogen by standard Schlenk techniques. Thin-layer chromatography (TLC) was carried out on 0.1 × 20 × 20 cm layers of silica gel, Fluka type GF254, on glass plates produced from aqueous slurries followed by drying in air at ca. 80 °C. NMR studies were carried out at 5.9 and 9.4 T (fields corresponding to 250 and 400 MHz ^{1}H NMR frequencies, respectively). Chemical shifts δ are given in parts per million (ppm) to high frequency (low field) of Ξ 100 MHz ($SiMe_4$) for ^{1}H (quoted ±0.05 ppm) and Ξ 32.083 971 MHz (nominally [$BF_3(OEt_2)$] in $CDCl_3$) for ^{11}B (quoted ±0.5 ppm), Ξ being as defined by McFarlane.[32] The chemical shifts were calibrated with solvent deuteron or residual proton resonances as internal secondary standards. Infrared spectra were recorded on a Perkin-Elmer FTIR 1600 spectrometer.

Synthesis of [NMe_4][*arachno*-B_9H_{12}-4,8-Br_2] 1. Dichloromethane (ca. 30 cm^3) was condensed into a 100 cm^3 round-bottomed flask, containing [NMe_4][*nido*-B_9H_{12}] (0.93 g, 5.1 mmol) and $HgBr_2$ (1.91 g, 5.3 mmol), attached to one end of an extractor. The mixture was allowed to warm to room temperature with stirring, during which time a gray precipitate formed. After ca. 1 h the product mixture was filtered, and the filtrate was reduced to dryness under vacuum. The resultant yellow solid was extracted into toluene and filtered with a second extractor, affording a gray-white powder, which was identified as [NMe_4]-[*arachno*-B_9H_{12}-4,8-Br_2] (compound **1**) (620 mg, 1.82 mmol, 36%). Removal of toluene from the filtrate allowed isolation of *anti*-[$B_{18}H_{22}$] as a very pale yellow solid (150 mg, 710 μmol, 18%). Diffusion of hexane into a solution of **1** in $CDCl_3$ allowed isolation of crystals suitable for X-ray analysis.

Synthesis of [*arachno*-B_9H_{13}-4-{$P(CCH)_3$}] 3. Diethyl ether (ca. 10 cm^3) was condensed into a two-necked round-bottomed flask containing a magnetic stirring bar and freshly prepared K[B_9H_{14}] (248 mg, 1.6 mmol). After dissolution, giving a clear solution, 1 equiv of HCl was condensed into the flask and stirring continued for 30 min. The compound [$P(CCH)_3$] (172 mg, 1.6 mmol) was then added against a flow of dinitrogen. The solution was stirred for a further 30 min and filtered in air, and the solvent was removed at ambient temperature on a rotary evaporator (water-pump pressure). The residue was redissolved in CH_2Cl_2 and applied to a preparative TLC plate, which was then developed with CH_2Cl_2/hexane (75:25). A single band observed under ultraviolet light (R_f 0.7) was removed from the plate and extracted with CH_2Cl_2, and the extract was evaporated, affording [*arachno*-B_9H_{13}-4-{$P(CCH)_3$}] (compound **3**), 133 mg, 0.61 mmol, 38%; infrared/cm^{-1} (KBr disk): υ(C−H) 1411w and 1398w; υ(C≡C) 2070vs; υ(B−H) 2519sh, 2535vs, 2551sh, and 2591m, υ(≡CH) 3251vs and 3270vs. Mass spectrometry (FAB): *m*/*e* 215 corresponding to the calculated envelope for $(M - 2H)^+$. NMR data are listed in Table 5.

Attempts to produce single crystals by slow diffusion of hexane into chloroform solutions of the compound were unsuccessful. However, rapid evaporation under a dinitrogen stream of a solution of the compound in Et_2O (ca. 0.5 cm^3 of a saturated solution in a 1 cm^3 sample tube under a nitrogen stream delivered through a Pasteur pipet) gave small, indeed very small, colorless single-crystal plates requiring a synchrotron X-ray radiation source for sufficient diffraction intensity for structural elucidation.

Synthesis of [*arachno*-B_9H_{13}-4-(NC_5H_5)] 5. Pyridine (470 μL, 580 μmol) was added to a stirred solution of [*arachno*-B_9H_{13}-4-(SMe_2)] (100 mg, 580 μmol) in CH_2Cl_2 (20 cm^3), effecting an immediate color change, from colorless to pale orange. Stirring was continued for 30 min, after which time the more volatile components were removed (rotary evaporator, 45 °C bath, water-pump pressure). Diffusion of hexane into a concentrated solution of the product in CH_2Cl_2 yielded dark tan-colored crystals of [*arachno*-B_9H_{13}-4-(NC_5H_5)] (compound **5**) of suitable quality for a single-crystal X-ray diffraction study (37 mg, 0.20 mmol, 35%).

Synthesis of [*arachno*-B_9H_{13}-4-(NH_2CH_2Ph)] 6. This compound was isolated as an unexpected minor product during an attempted synthesis of [$(PhCN)_2PtB_8H_{12}$] from K[B_9H_{14}] and [*trans*-$PtCl_2(NCPh)_2$]. Thus, [*trans*-$PtCl_2(NCPh)_2$] (300 mg, 635 μmol) was added to a solution of K[B_9H_{14}] (290 mg, 2.0 mmol) in methanol (ca. 15 cm^3), and the mixture was stirred under dinitrogen for 30 min. Unreacted [$PtCl_2$-$(NCPh)_2$] (250 mg) was then retrieved from the reaction mixture by filtration. The amber-colored filtrate was subjected to TLC separation (80:20 CH_2Cl_2/hexane). The only identifiable product from the reaction, [*arachno*-B_9H_{13}-4-(NH_2CH_2Ph)] (compound **6**), appeared as a chromatographic band (R_f 0.65) that weakly fluoresced under ultraviolet irradiation. Evaporation of the CH_2Cl_2 extract of this band gave trace quantities of compound **6** as a colorless solid. Slow diffusion of hexane into a CH_2Cl_2 solution of the compound yielded colorless single crystals suitable for the single-crystal X-ray diffraction experiments.

Calculational Method. Structures were initially optimized with the STO-3G and 6-31G* basis sets by the standard ab initio methods package Gaussian 98.[33] Final optimizations, frequency analyses to confirm true minima, and GIAO nuclear shielding predictions were performed by B3LYP methodology, also as incorporated in the Gaussian 98 and with the 6-31G* basis set. Gas-phase nuclear shielding predictions were calibrated to the ^{11}B NMR chemical-shift scale via a

(29) Graybill, M.; Ruff, J. K.; Hawthorne, M. F. *J. Am. Chem. Soc.* **1961**, *83*, 2669.
(30) Voskuil, W.; Arens, J. F. *Rec. Trav. Chim.* **1964**, 1301.
(31) Graybill, B. M.; Pitochelli, A. R.; Hawthorne, M. F. *Inorg. Chem.* **1962**, *1*, 626.
(32) McFarlane, W. *Proc. R. Soc. London* **1986**, *A306*, 185.
(33) Frisch, M. J.; Trucks, G. W.; Schlegel, H. B.; Scuseria, G. E.; Robb, M. A.; Cheeseman, J. R.; Zakrzewski, V. G.; Montgomery, J. A., Jr.; Stratmann, R. E.; Burant, J. C.; Dapprich, S.; Millam, J. M.; Daniels, A. D.; Kudin, K. N.; Strain, M. C.; Farkas, O.; Tomasi, J.; Barone, V.; Cossi, M.; Cammi, R.; Mennucci, B.; Pomelli, C.; Adamo, C.; Clifford, S.; Ochterski, J.; Petersson, G. A.; Ayala, P. Y.; Cui, Q.; Morokuma, K.; Malick, D. K.; Rabuck, A. D.; Raghavachari, K.; Foresman, J. B.; Cioslowski, J.; Ortiz, J. V.; Baboul, A. G.; Stefanov, B. B.; Liu, G.; Liashenko, A.; Piskorz, P.; Komaromi, I.; Gomperts, R.; Martin, R. L.; Fox, D. J.; Keith, T.; Al-Laham, M. A.; Peng, C. Y.; Nanayakkara, A.; Gonzalez, C.; Challacombe, M.; Gill, P. M. W.; Johnson, B.; Chen, W.; Wong, M. W.; Andres, J. L.; Gonzalez, C.; Head-Gordon, M.; Replogle, E. S.; Pople, J. A. *Gaussian 98*, Revision A.7; Gaussian, Inc.: Pittsburgh, PA, 1998.

Table 1. Crystal Data and Structure Refinement for $[NMe_4][B_9H_{12}Br_2]$ **1**, $K[B_9H_{14}]$ **2**, $[B_9H_{13}P(C_2H)_3]$ **3**, $[B_9H_{13}NHEt_2]$ **4**, $[B_9H_{13}NC_5H_5]$ **5**, $[B_9H_{13}NH_2(CH_2Ph)]$ **6**, and $[B_9H_{13}NCMe]$ **9**

compound	**1**	**2**	**3**	**4**
empirical formula	$C_4H_{24}B_9Br_2N$	$H_{14}B_9K$	$C_6H_{16}B_9P$	$C_4H_{24}B_9N$
formula weight	343.35	150.50	216.45	183.53
temp/K	146(2)	143(2)	200(2)	150(2)
diffractometer	Stoe STADI 4	Siemens P4	Bruker Smart CCD	Nonius Kappa CCD
source and λ/Å	Cu Kα 1.54184	Mo Kα 0.71073	synchrotron 0.6942	Mo Kα 0.71073
crystal system	monoclinic	monoclinic	monoclinic	orthorhombic
space group	$P2_1/c$	$P2_1/c$	$P2_1/c$	Pbca
a/Å	8.8043(4)	7.717(2)	6.0434(7)	9.5057(1)
b/Å	18.4412(7)	11.674(2)	18.628(2)	12.8371(2)
c/Å	10.0523(4)	10.054(2)	12.6874(15)	20.9018(3)
β/deg	99.256(4)	95.091(3)	92.062(2)	90
V/Å^{-3}	1610.86(12)	902.2(3)	1427.4(3)	2550.55(6)
Z	4	4	4	8
D (calc)/Mg m^{-3}	1.416	1.108	1.007	0.956
abs coeff/mm^{-1}	6.089	0.496	0.154	0.044
cryst size/mm	0.53 × 0.36 × 0.19	0.30 × 0.20 × 0.20	0.25 × 0.11 × 0.01	0.20 × 0.20 × 0.20
F(000)	680	312	448	800
θ range for data collcn/deg	2.40−32.29	2.65−32.59	2.14−25.99	2.9−26
index ranges	$-10 \le h \le 10$, $0 \le k \le 21$, $0 \le l \le 11$	$-11 \le h \le 10$, $-17 \le k \le 17$, $0 \le l \le 15$	$-7 \le h \le 7$, $-23 \le k \le 23$, $-16 \le l \le 16$	$-11 \le h \le 11$, $-15 \le k \le 15$, $-25 \le l \le 25$
reflcns collected	2584	6063	11 724	25 229
indep reflcns	2584 (Rint = 0.0000)	3022 (Rint = 0.034)	3008 [R(int) = 0.029]	2498 [R(int) = 0.058]
max, min transmission	0.349, 0.162	0.874, 0.695	0.998, 0.963	0.991, 0.991
data/restraints/parameters	2584/0/239	3022/0/147	3008/0/197	2498/0/186
goodness-of-fit on F^2	1.052	1.06	1.11	1.063
final R indices [$I > 2\sigma(I)$] R_1	0.042	0.033	0.040	0.039
final R (all data) $wR_2(F^2)$	0.1118	0.070	0.103	0.106
largest diff peak and hole/e Å^{-3}	0.88, −0.75	0.33, −0.17	0.50, −0.20	0.18, −0.12

compound	**5**	**6**	**9**
empirical formula	$C_5H_{18}B_9N$	$C_7H_{22}B_9N$	$C_2H_{16}B_9N$
formula weight	189.49	217.55	151.45
temp/K	160(2)	150(2)	150(2)
diffractometer	Siemens Smart CCD	Nonius Kappa CCD	Nonius Kappa CCD
source and λ/Å	Cu Kα 1.54184	Mo Kα 0.71073	Mo Kα 0.71073
crystal system	triclinic	orthorhombic	monoclinic
space group	$P\bar{1}$	$P2_12_12_1$	$P2_1$
a/Å	5.7787(4)	10.1178(3)	5.6183(11)
b/Å	10.1992(7)	5.6413(1)	9.0867(18)
c/Å	10.4677(8)	24.5250(8)	9.844(2)
α/deg	87.154(2)	90	90
β/deg	76.907(2)	90	90.41(3)
γ/deg	84.296(2)	90	90
V/Å^{-3}	597.70(7)	1399.83(7)	502.56(17)
Z	8	4	2
D (calc)/Mg m^{-3}	1.053	1.032	1.001
abs coeff/mm^{-1}	0.337	0.050	0.045
cryst size/mm	0.53 × 0.36 × 0.19	0.35 × 0.09 × 0.06	0.27 × 0.17 × 0.13
F(000)	200	464	160
θ range for data collcn/deg	2.17−44.50	3.20−26.00	4.14−26.00
index ranges	$-7 \le h \le 7$, $-13 \le k \le 13$, $-13 \le l \le 13$	$-10 \le h \le 12$, $-6 \le k \le 6$, $-29 \le l \le 30$	$-6 \le h \le -6$, $-10 \le k \le 11$, $-11 \le l \le 12$
reflcns collected	7237	2726	5544
indep reflcns	2671(Rint = 0.024)	2446(Rint = 0.072)	1045(Rint = 0.048)
max, min transmission		0.983, 0.997	0.994, 0.988
data/restraints/parameters	2671/4/189	2726/0/207	1045/0/108
goodness-of-fit on F^2	1.055	1.049	1.09
final R indices [$I > 2\sigma(I)$] R_1	0.0412	0.0395	0.040
final R (all data) $wR_2(F^2)$	0.111	0.0930	0.110
largest diff peak and hole/e Å^{-3}	0.23,−0.17	0.18, −0.19	0.15, −0.13

prediction on diborane, which is taken to have a gas-phase $\delta(^{11}B)$ value of −16.6 ppm with respect to $[BF_3(OEt_2)]$.

X-ray Crystallography. Single crystals of compounds **1**, **2**, **3**, **5**, and **6** were obtained as described above. Crystals of [*arachno*-B_9H_{13}-4-$NHEt_2$)] **4** were obtained from acetonitrile solutions at −10 °C by the technique of overlayering with diethyl ether. Data collection and refinement details are listed in Table 1. The structures were solved by direct methods and refined by full-matrix least-squares methods on all measured F^2 values, with a weighting scheme $w^{-1} = \sigma^2(F_o^2) + (aP)^2 + (bP)$, where $P = (F_o^2 + 2F_c^2)/3$. Residuals were defined by $R_1 = \Sigma||F_o| - |F_c||/\Sigma|F_o|$, $wR_2 = \sqrt{[\Sigma w(F_o^2 - F_c^2)^2/\Sigma w(F_o^2)^2]}$. Programs consisted of standard control software for the diffractometers, local programs, and members of the SHELX family for **1**, **3**, **4**, **5**, **6**,[34a] **9**,[34b] and **2**.[35] The very thin plates (0.01 mm) that were obtained for

(34) (a) Sheldrick, G. M., SHELX97, University of Göttingen, Germany, 1997. (b) Sheldrick, G. M. SHELXTL manual, Bruker AXS, Madison, WI, 1994 and 1998.

(35) See, for example, Bould, J.; Rath, N. P.; Barton, L. *Inorg. Chem.* **1996**, *35*, 35. Data reduction was done per XSCANS, Siemens Analytical Instruments, Madison, WI, 1994, and refinement per Sheldrick, G. M., Siemens Analytical X-ray Division, Madison, WI, 1994.

Table 2. Selected Interatomic Distances[a] for $[NMe_4][B_9H_{12}Br_2]$ (**1**) and KB_9H_{14} (**2**) Together with Calculated Distances for the $[B_9H_{14}]^-$ Anion

	1	2	calc[b]		1	2	calc[b]
Br4−B4	2.018(5)			Br8−B8	2.006(5)		
B1−B2	1.778(6)	1.787(2)	1.796	B2−B3	1.798(7)	1.795(2)	1.796
B1−B3	1.786(6)	1.787(2)	1.786	B2−B5	1.768(7)	1.798(2)	1.794
B1−B4	1.724(7)	1.732(2)	1.733	B2−B6	1.710(7)	1.713(2)	1.706
B1−B5	1.731(6)	1.733(2)	1.731	B2−B7	1.761(7)	1.765(2)	1.757
B1−B9	1.750(6)	1.740(2)	1.728	B3−B7	1.732(6)	1.744(2)	1.734
B3−B8	1.761(6)	1.772(2)	1.780	B3−B9	1.769(7)	1.790(2)	1.782
B4−B5	1.952(7)	1.913(2)	1.931	B4−B9	1.868(7)	1.873(2)	1.881
B5−B6	1.785(7)	1.816(2)	1.797	B6−B7	1.790(7)	1.786(2)	1.778
B7−B8	1.994(7)	2.004(2)	2.023	B8−B9	1.876(7)	1.885(2)	1.878
B1−H1	1.14(4)	1.092(14)		B2−H2	1.05(4)	1.107(14)	
B3−H3	1.11(4)	1.07(2)		B4−H4a[c]		1.101(14)	
B4−H4b[c]		1.085(14)		B5−H5	1.05(4)	1.080(14)	
B5−H56	1.16(4)	1.28(2)		B6−H6	1.08(4)	1.05(2)	
B6−H56	1.25(5)	1.27(2)		B6−H67	1.22(4)	1.20(2)	
B7−H7	1.17(4)	1.07(2)		B7−H67	1.27(5)	1.32(2)	
B8−H8a[c]		1.070(14)		B8−H8b[c]		1.10(2)	
B8−H89	1.40(6)	1.34(2)		B9−H9	1.12(5)	1.10(2)	
B9−H89	1.20(7)	1.21(2)					

[a] Interatomic distances are given in angstroms, with s.u's in parentheses. [b] Calculated distances for $[B_9H_{14}]^-$ anion. Data were taken from ref 19. [c] H4a and H8a denote *endo*-terminal H atoms and H4b and H8b denote *exo*-terminal H atoms in compound **2**.

compound **3** necessitated the use of synchrotron radiation for sufficient diffracted-beam intensity for structural analysis. The cation in **1** exhibited disorder, which was resolved as two different orientations of the methyl groups in the ratio 67:33.

Results and Discussion

Reaction of $[NMe_4][nido\text{-}B_9H_{12}]$ with $HgBr_2$ in CH_2Cl_2, followed by toluene extraction of the *anti*-$B_{18}H_{22}$ product, leaves a toluene-insoluble white solid. ^{11}B and ^1H NMR spectroscopy showed that this solid consists of a mixture of two borane compounds. Yields of these two compounds are variable, but in one experiment, we obtained the main component sufficiently in excess to enable its crystallization as a pure species in 36% yield. This enabled its full characterization as off-white, air-stable $[NMe_4][arachno\text{-}B_9H_{12}\text{-}4,8\text{-}Br_2]$ (compound **1**, structure **VI**) by a single-crystal X-ray diffraction analysis (Tables 2 and 3 and Figure 1), together with ^{11}B and ^1H NMR spectroscopy (Table 4). The bromine substitution is observed to have occurred at two of the more prominent crown point open-face sites, B4 and B8, rather than at open-face notch positions or at off-face positions, and it is of interest that the bromination occurs so specifically at these sites and in reasonable yield. Here, incidentally, it may be noted that we have a report that the anion of compound **1** may be produced more conveniently by direct bromination of the *arachno*-$[B_9H_{14}]^-$ anion in CH_2Cl_2 solution.[36] A stoichiometry may be written as follows:

$$[B_9H_{12}]^- + HgBr_2 \rightarrow [B_9H_{12}Br_2]^- + Hg\downarrow$$

Interestingly, as discussed below, the $[arachno\text{-}B_9H_{12}\text{-}4,8\text{-}Br_2]^-$ anion in compound **1** has an open-face hydrogen-atom disposition different from that originally reported[16b,c] for the unsubstituted $[arachno\text{-}B_9H_{14}]^-$ anion as its Cs^+ salt (compound **7**).

Contemporaneously, in unrelated experiments, our attempts to crystallize $[Cd(B_5H_8)_2]$ from solutions in tetrahydrofuran that also contained KCl led to the serendipitous isolation of high-quality crystals of $K[arachno\text{-}B_9H_{14}]$ (compound **2**).[28] We were thence also able to examine this in a low-temperature X-ray diffraction study of a single crystal (Tables 1−3 and Figure 1). Selected interatomic distances (Table 2) and angles (Table 3) for both **1** and **2** are listed together to aid comparison. The borane cluster geometries for the $[arachno\text{-}B_9H_{12}\text{-}4,8\text{-}Br_2]^-$ and $[arachno\text{-}B_9H_{14}]^-$ anions in compounds **1** and **2** are seen to be isostructural as far as the boron skeleton and attached hydrogen

Table 3. Selected Interatomic Angles[a] for $[NMe_4][B_9H_{12}Br_2]$ (**1**) and KB_9H_{14} (**2**)

	1	2		1	2
B4−B1−B5	68.8(3)	67.00(7)	B4−B1−B9	65.0(3)	65.29(7)
B5−B1−B9	119.4(4)	118.83(8)	B4−B1−B3	113.0(3)	114.14(8)
B5−B1−B3	108.9(3)	110.29(8)	B9−B1−B3	60.0(3)	60.98(7)
B4−B1−B2	119.5(3)	118.37(8)	B5−B1−B2	60.5(3)	61.41(6)
B9−B1−B2	114.6(3)	114.47(8)	B3−B1−B2	60.6(3)	60.29(6)
B6−B2−B7	62.1(3)	61.80(7)	B6−B2−B1	109.8(3)	109.35(8)
B7−B2−B1	105.9(3)	105.20(8)	B6−B2−B3	110.4(3)	110.95(9)
B7−B2−B3	58.2(3)	58.65(7)	B1−B2−B3	59.9(3)	59.84(6)
B6−B2−B5	61.7(3)	62.23(7)	B7−B2−B5	107.6(3)	107.49(8)
B1−B2−B5	58.4(3)	57.81(6)	B3−B2−B5	106.8(3)	107.02(7)
B7−B3−B8	69.9(3)	69.49(7)	B7−B3−B1	106.7(3)	106.12(8)
B8−B3−B1	111.1(3)	111.87(8)	B7−B3−B9	118.2(4)	115.32(8)
B8−B3−B9	64.2(3)	63.89(7)	B1−B3−B9	59.0(3)	58.22(6)
B7−B3−B2	59.8(3)	59.81(7)	B8−B3−B2	119.1(3)	120.29(8)
B1−B3−B2	59.5(3)	59.87(6)	B9−B3−B2	112.7(3)	111.67(7)
B1−B4−B9	58.2(3)	57.55(6)	B1−B4−B5	55.8(3)	56.52(6)
B9−B4−B5	103.8(3)	104.32(8)	B1−B4−Br4	119.9(3)	
B5−B4−Br4	119.5(3)		B9−B4−Br4	116.8(3)	
B5−B4−Br4		117.9(8)	B1−B4−H4a[b]		112.7(8)
			B9−B4−H4a[b]		118.3(8)
B1−B5−B2	61.1(3)	60.78(6)	B1−B5−B6	108.5(3)	107.16(8)
B2−B5−B6	57.5(3)	56.59(6)	B1−B5−B4	55.4(3)	56.48(6)
B2−B5−B4	108.7(3)	109.07(8)	B6−B5−B4	118.3(3)	117.01(9)
B2−B6−B7	60.4(3)	60.53(7)	B2−B6−B5	60.7(3)	61.19(7)
B7−B6−B5	105.6(3)	105.80(8)			
B2−B7−B6	57.6(3)	57.68(7)	B3−B7−B8	55.9(3)	55.92(7)
B2−B7−B8	109.4(3)	110.19(8)	B6−B7−B8	118.4(3)	121.11(8)
B3−B8−B9	58.1(3)	58.52(7)	B3−B8−B7	54.5(3)	54.59(6)
B9−B8−B7	101.8(3)	100.27(8)	B3−B8−Br8	112.1(3)	
B9−B8−Br8	115.3(3)		B7−B8−Br8	122.9(3)	
B9−B8−H8a[b]		113.2(8)	B3−B8−H8a[b]		108.2(8)
			B7−B8−H8a[b]		124.4(8)
B1−B9−B3	61.0(3)	60.80(6)	B1−B9−B4	56.8(3)	57.16(6)
B3−B9−B4	107.1(3)	107.48(8)	B1−B9−B8	107.5(3)	108.79(8)
B3−B9−B8	57.7(3)	57.59(6)	B4−B9−B8	111.5(3)	114.32(8)

[a] Interatomic angles are given in degrees, with s.u's in parentheses. [b] H4a and H8a denote *endo*-terminal H atoms and H4b and H8b denote *exo*-terminal H atoms in compound **2**.

(36) Brellochs, B. *Abstracts, Tenth International Conference on Boron Chemistry*, Durham, U.K., July 1999; Paper PA-13.

Table 4. ^{11}B and ^{1}H NMR Chemical Shift Data[a] for $[NMe_4][B_9H_{12}Br_2]$ in CD_2Cl_2 Solution

assignment	$\delta(^{11}B)$ (300 K)	J(B–H)/Hz	(^{11}B–^{11}B) COSY	$\delta(^{1}H)$ (300 K)	$\delta(^{1}H)$ (185 K)	(^{1}H–^{1}H) (185 K)	COSY (203 K)	$\delta(^{11}B)$ $[B_9H_{14}]^-$ IGLO calcd[b]
(5), (7)	+3.5(2)	146	(1,2,3)s, (6,8)w	+3.19(2)	+3.10(2)			+13.8, −10.5 (+1.7)
(6)	−4.7	151	(1)s	+2.87	+2.89	μ\{(4,5),(4,9)\}w	μ\{(4,5),(4,9)\}w	−7.0
(1), (3)	−9.1(2)	128	(1,5,6,7,8,9)s	+2.31(2)	+2.15(2)		(1)m, (2,3)s, (6,8)s	+8.7, −24.9 (−8.1)
(4), (8)	−15.9(2)	*c*	(7)s, (5,9)w	−0.36(2)	+1.80(2)	μ(6,7)s		−24.0, −25.4 (−24.7)
(9)	−30.1	142	(2,3,6,8)s	+1.09	+0.95			−33.1
(2)	−48.1	150	(2,3,4,5,9)s	−0.36	−0.54		(2,3)m, μ\{(4,5),(4,9)w	−52.5
H(8,9)				−0.36(3)	−1.31	(6,8)s		
H(6,7), (5,6)					−2.53(2)	(4)w	(4)w	
$N(CH_3)_4$				+3.06	+3.19			

[a] Chemical shift data are given in parts per million. [b] IGLO calculated chemical shifts for *arachno*-$[B_9H_{14}]^-$ anion, with mean chemical shifts in parentheses, are given for comparison. Data were taken from ref 19. [c] Site of bromine substituents. ^{11}B resonance sharpens on proton decoupling, indicating unresolved coupling to *endo*-terminal protons.

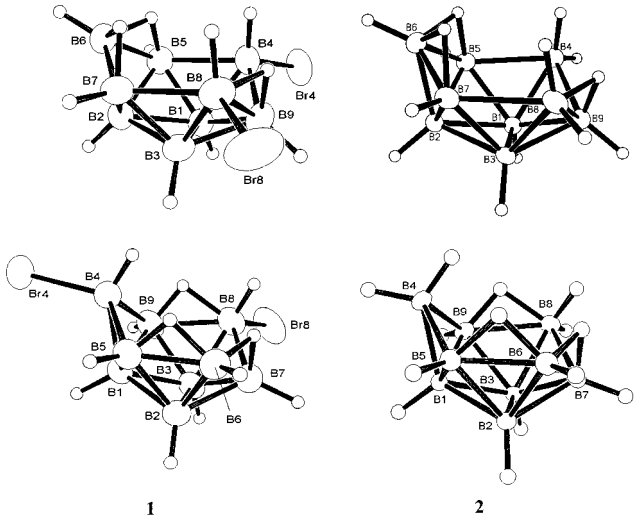

1 **2**

Figure 1. Crystallographically determined molecular structures for the [*arachno*-4,8-$Br_2B_9H_{12}]^-$ anion in $[NMe_4]$[*arachno*-4,8-$Br_2B_9H_{12}$] **1** and the [*arachno*-$B_9H_{14}]^-$ anion in K[*arachno*-B_9H_{14}] **2**, drawn with 50% probability ellipsoids for **1** and 40% for **2**, with hydrogen atoms shown as small circles of arbitrary radii.

atoms are concerned: for both species the majority of equivalent interatomic distances and angles are the same within experimental error. The positions of the boron atoms and the *exo*-hydrogen atoms are also very similar to those reported from the earlier room-temperature study of $Cs[B_9H_{14}]$ (compound **7**, structure **V**).[16b,c] Significantly, however, the anions in **2** and **7** do differ; specifically, in the positioning and nature of the five inner-sphere *endo*-terminal and bridging hydrogen atoms. Thus the $[B_9H_{14}]^-$ anion in compound **7** had previously been analyzed to have the {2×μ-H, 3×*endo*} configuration of structure **V**, whereas both the dibrominated anion in **1** and, more importantly, the $[B_9H_{14}]^-$ anion in **2** have the mutually analogous {3×μ-H, 2×*endo*} configurations (structures **VI** and **VII**, respectively). The question therefore arises as to whether **V** or **VII** is the ground-state structure for the anion, particularly so as the older, but now ostensibly unique, {2×μ-H, 3×*endo*} configuration **V** is generally quoted as being the definitive structural motif. At this point, it is interesting to note that a relatively recent report of the structure of the [*arachno*-B_9H_{11}-6,7,8-$Cl_3]^-$ anion indicates that this species too exhibits the {3×μ-H, 2×*endo*} disposition derived for **1** and **2**;[37] additionally, this disposition has now also been derived for the Cs^+ salt of **7** from its low-temperature diffraction data.[23] Similarly, a structural type that is a variant of the [*arachno*-B_9H_{13}-4-L] system, the series of compounds [*arachno*-B_9H_{13}-4-L] with the ligand now on the notched 5-position rather than the exposed 4-position, also shows the same {3×μ-H, 2×*endo*} configuration (structure **X**).[21] Neutral heteroborane adducts such as [*arachno*-6-NB_8H_{11}-4-L] also have closely related configurations.[38]

The fluxionality of these anions may have significance with respect to the {3×μ-H, 2×*endo*} versus {2×μ-H, 3×*endo*} structural motif. The $[B_9H_{14}]^-$ anion is fluxional with regard to complete exchange of the five inner-sphere hydrogen atoms, with the fluxional process apparently having a very low activation energy. Thus a very rapid exchange of these five hydrogen atoms among inner-sphere bridging and *endo*-terminal sites on the open face engenders on time-average an effective C_{3v} symmetry for the remaining $\{B_9H_9\}$ cluster unit and a resulting 3:3:3 ^{11}B NMR relative-intensity pattern, with $\delta(^{11}B)$ values ca. −6.6, −19.7, and −21.6 ppm.[39] On the assumption that the static structure has a {3×μ-H, 2×*endo*} open-face configuration analogous to that of the $[B_9H_{13}L]$ derivatives established below, which is reasonable in that $[H]^-$ is an effective two-electron donor to the cluster, then these three mean chemical shift values are reasonably derived from the averaging of the shifts for the 1,2,3, the 4,6,8, and the 5,7,9 positions, generating the idea that the BH_2 vertex at position 4 would have a $\delta(^{11}B)$ value of ca. −6 ppm. This experimental perception concurs with the Hofmann/Schleyer calculations[19] of the ^{11}B chemical shifts, based on the structure of the $[B_9H_{14}]^-$ ion in which all the B atoms are unique (Table 4) and in which the $\delta(^{11}B)$ value for the BH_2(4) unit in the (static) anion is predicted to be −7.0 ppm on the basis of the IGLO calculations. The fluxionality cannot be arrested down to 203 K,[22d] implying $\Delta G^{\ddagger}$ < ca. 30 kJ mol^{-1}. The dibromo species **1** reported herein is also similarly fluxional, although probably with a somewhat higher activation energy, as incipient NMR peak separation is observed with an implied coalescence temperature of ca. 233 K, giving an upper limit for $\Delta G^{\ddagger}_{233}$ of *ca*. 40 kJ mol^{-1}. The manifestation of this fluxonality is that although the $[B_9H_{12}Br_2]^-$ anion in the solid-state structure of compound **1** has no symmetry, a 2:2:2:1:1:1 ^{11}B NMR relative-intensity pattern is observed at all temperatures (Table 4). The fluxionality gives on time-average an effective plane of symmetry with respect to the Br substituents at positions 4 and 8, which renders each of the pairs of atoms B5/B7, B1/B3, and B4/B8 equivalent in

(37) Hamilton, E. J. M.; Liu, J.; Meyers, E. A.; Shore, S. G. *Abstracts of the 213th National Meeting of the American Chemical Society*, Paper INOR-313; San Francisco, CA, April 1997.

(38) Price, C.; Dörfler, U.; Kennedy, J. D.; Thornton-Pett, M. *Acta Crystallogr.* **2000**, C*56*, 600.

(39) Schaeffer, R.; Sneddon, L. G. *Inorg. Chem.* **1972**, *11*, 3102.

Chart 4

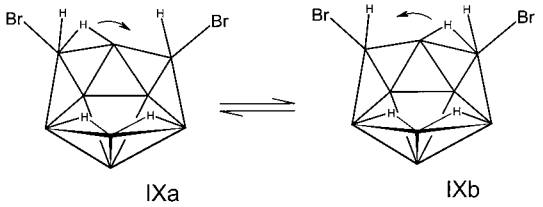

the pairs indicated. If the mean of the IGLO-calculated δ (^{11}B) values of Hofmann[19] are taken for each of the B5/B7 and B1/B3 pairs in the $[B_9H_{14}]^-$ ion, they compare well to the observed values for the $[B_9H_{12}Br_2]^-$ anion in compound **1**. With the imposition of a reasonably estimated upfield shift of ca. +10 ppm[40] arising from the bromine substituents on B4 and B8 in $[B_9H_{12}Br_2]^-$, the experimental and calculated shifts also compare satisfactorily (Table 4). Our attempts to perform ab initio calculations and thus derive gauge-invariant atomic orbital (GIAO) calculated chemical shift values for the $[B_9H_{12}Br_2]^-$ anion have so far been unsatisfactory, possibly because of relativistic effects due to the heavier bromine atom not being taken into account in the B3LYP/6-31G* model employed.[41]At lower temperatures, however, the five inner-sphere hydrogen atoms of $[B_9H_{12}Br_2]^-$ do exhibit a 2:2:1 ^{1}H NMR relative intensity pattern, rather than the five equal resonances otherwise expected from consideration of the asymmetric solid-state structure. This now implies a two-stage fluxionality: one with a higher activation energy, involving exchange among all five of the inner-sphere hydrogen atoms, and a residual lower-energy process involving the interchange of character between *endo* and bridging of the two inner-sphere hydrogen atoms associated with the B6B7B8 notch (structures **IXa** and **IXb** in Chart 4). A similar low-energy process is apparent for the isoelectronic *arachno* nine-vertex $[4\text{-}SB_8H_{11}]^-$, $[4\text{-}NB_8H_{12}]^-$, and $[4\text{-}CB_8H_{13}]^-$ anions,[42−44] which have {S}, {NH}, and {CH_2} units at position 6 instead of the {BH(μ-H)$_2$} unit of Figure 1. The behavior is also related somewhat to the well-discussed *endo* hydrogen-atom behavior at the BH_2, 1-position of neutral *arachno*-B_5H_{11}.[45] The same two-hydrogen fluxional process also seems likely in the B6B7B8 notch of the *arachno*-type nine-vertex metallaboranes such as $[L_2PtB_8H_{12}]$ and $[L_2PdB_8H_{12}]$,[46] with original suppositions[13a,47] about the dual partial bridging character of these two inner-sphere hydrogen atoms in these species having now also to be revised appropriately. This latter type of fluxionality applies also to the B6B7B8 notch of the [*arachno*-B_9H_{13}-4-L] species discussed below. There is also relevance here to the behavior of *nido*- and *arachno*-octaborane species, viz., neutral B_8H_{12} and neutral B_8H_{14} and the $[B_8H_{11}]^-$ and $[B_8H_{13}]^-$ anions.[48] In all these species, including the $[B_9H_{12}Br_2]^-$ anion, this residual two-hydrogen fluxional process is of very low energy and is not quenched at low temperatures.

The sum of the above evidence clearly stimulates a reassessment of the original {2×μ-H, 3×*endo*} configuration **V** derived for the $[B_9H_{14}]^-$ anion in Cs$[B_9H_{14}]$. There now seems little doubt that the $[B_9H_{14}]^-$ anion {3×μ-H, 2×*endo*} configuration **VII** is in fact the ground state and that it also obtains in the crystals of compounds **2** and **7**. Although the ready fluxionality suggests very low energy differences between different hydrogen-atom configurations, so that in principle configuration **V** could arise from the different crystal packing forces in the Cs^+ versus K^+ salts **7** and **2**, it seems reasonable that the apparently different structure arises almost certainly from the inherently larger experimental error present in the earlier room-temperature studies rather than, for example, differences in crystal packing forces due to the effects of the differing Cs^+ and K^+ counterions in the two determinations. Additionally, of course, the {3×μ-H, 2×*endo*} configuration is additionally supported by the results of Huffman's low-temperature diffraction study on compound **7** itself.[23]

The [B_9H_{13}-4-L] species are also similarly fluxional when L is an anionic ligand, such as the $\{NCS\}^-$ or $\{(NC)BH_3\}^-$ moiety.[22d] In this regard, of course, the ligand L is effectively H^- in the $[B_9H_{14}]^-$ anion discussed above. The NMR peak-coalescence temperature of 243 K for the [*arachno*-B_9H_{13}-4-(NCS)]$^-$ species[22d] gives $\Delta G^{\ddagger}_{243}$ *ca.* 43 kJ mol^{-1}, similar to that of the $[B_9H_{12}Br_2]^-$ anion reported herein. As mentioned in the Introduction, a similar {3×μ-H, 2×*endo*} arrangement of inner-sphere hydrogen atoms to those of $[B_9H_{12}Br_2]^-$ and $[B_9H_{14}]^-$ anions in compounds **1** and **2** was noted some time ago in structural studies of the *arachno*-$[B_9H_{13}(NCS)]^-$ anion in its $[N(PPh_3)_2]^+$ salt (compound **8**, structure **VIII**).[20] For this last anion, the results of extended-Hückel molecular-orbital (MO) calculations were taken to support the idea that this different arrangement would arise in $[B_9H_{13}L]$ species where L is a π-acceptor ligand such as $[NCS]^-$, as distinct from a pure σ-bonded ligand such as the effective $[H]^-$ ligand in the unsubstituted $[B_9H_{14}]^-$ anion itself. These conclusions, however, were based on a comparison with the ambient-temperature structural determination of Cs$[B_9H_{14}]$ (compound **7**)[16b,c] that had derived configuration **V** for the $[B_9H_{14}]^-$ anion, whereas, as discussed above, structure **VII** is now best regarded as the most reasonable for $[B_9H_{14}]^-$, and so the π-acceptor character of the $[NCS]^-$ versus the H^- ligand is not so fundamentally decisive in this case. The B−μ-H−B moieties in the anions in **1** and **2** show some asymmetry, as has been observed often in borane chemistry[49] and as can be seen from the derived B−μ-H distances. In each case, the single hydrogen bridge at B8B9 shows more asymmetry than the pair of adjacent bridges at B5B6 and B6B7; this is perhaps expected, as it is in the most asymmetric environments in both **1** and **2**. The interboron distances for the pair of anions are quite unexceptional. The longest of these are B4−B5 and B7−B8: interestingly, these long values of 1.953(7) and 1.994(7) Å, respectively, approach the long *nido*-decaboranyl "gunwale" distances of ca. 2.0 Å.[50]

(40) Heřmánek, S. *Chem Rev.* **1992**, *92*, 325.
(41) Bühl, M.; Kaupp, M.; Malkina, O. L.; Malkin, V. G. *J. Comput. Chem.* **1999**, *20*, 91.
(42) Baše, K.; Wallbridge, M. G. H.; Fontaine, X. L. R.; Greenwood, N. N.; Jones, J. H.; Kennedy, J. D.; Štíbr, B. *Polyhedron* **1989**, *8*, 2089.
(43) Baše, K.; Plešek, J.; Heřmánek, S.; Huffman, J.; Ragatz, P.; Schaeffer, R. *J. Chem. Soc., Chem. Commun.* **1975**, 934.
(44) Wille, A. E.; Plešek, J.; Holub, J.; Štíbr, J.; Carroll, P. J.; Sneddon, L. G. *Inorg. Chem.* **1996**, *35*, 5342.
(45) (a) Leach, J. B.; Onak, T. P.; Spielman, J.; Rietz, R. R.; Schaeffer, R.; Sneddon, L. G. *Inorg. Chem.* **1970**, *9*, 2170. (b) Rietz, R. R.; Schaeffer, R.; Sneddon, L. G. *J. Am. Chem. Soc.* **1970**, *92*, 3414.
(46) Londesborough, M. G. S.; Kilner, C. A.; Thornton-Pett, M.; Kennedy, J. D. Manuscript in preparation.
(47) Kennedy, J. D. *Prog. Inorg. Chem.* **1986**, *34*, 211.
(48) (a) Condick, P. N.; Fox, M. A.; Greatrex, R.; Ormsby, D. L. *Spec. Publ. R. Soc. Chem.* **2000**, *253*, 179. (b) Tebben, A. J.; Ji, G.; Williams, R. E.; Bausch, J. W. *Inorg. Chem.* **1998**, *37*, 2189. (c) Lipscomb, W. N. *Pure Appl. Chem.* **1977**, *49*, 701. (c) Hall, J. H., Jr.; Dixon, D. A.; Kleier, D. A.; Halgren, T. A.; Brown, L. D.; Lipscomb, W. N. *J. Am. Chem. Soc.* **1975**, *97*, 4202.
(49) Beaudet, R. A. *Mol. Struct Energ.* **1988**, *5*, 417.
(50) Tippe, A.; Hamilton, W. C. *Inorg. Chem.* **1969**, *8*, 464.

Table 5. ^{11}B, ^{1}H, and ^{31}P NMR Chemical Shift Data for $[B_9H_{13}P(C_2H)_3]$ (**3**) in CD_2Cl_2 Solution at 300 K along with Calculated ^{11}B Chemical Shifts and Comparison NMR Data[a]

	$[B_9H_{13}P(C_2H)_3]$ (**3**)				$[B_9H_{13}NCS]$ (**8**)		$[B_9H_{13}NCMe]$ (**9**)	
assignment	$\delta(^{11}B)$ GIAO calcd[b]	$\delta(^{11}B)$ exptl	J(B–H)/Hz	$\delta(^{1}H)$	$\delta(^{11}B)$ GIAO calcd[b]	$\delta(^{11}B)$ exptl	$\delta(^{11}B)$ GIAO calcd[b]	$\delta(^{11}B)$ exptl
(1)	+5.9	+4.1	141	+3.12[c]	+3.7	+4.2	+6.1	+5.6
(2), (3)	−49.6, −25.3 (−36.8)	−38.6	139	+0.56(2)	−47.3, −28.0 (−38.8)	−38.3	−49.8, −25.3 (−37.5)	−38.3
(4)	−33.6	−34	*d*	−0.30	−22.7	−22.0	−32.1	−27.0
(5), (9)	−6.0, −20.6 (−15.2)	−13.3	141	+2.07(2)	−10.9, −33.7 (−17.8)	−16.4	−6.0, −20.6 (−13.3)	−14.0
(6), (8)	−12.4, −26.0 (−18.8)	−22.7	142	+1.98(2), +0.12(2)	+3.3, −6.2 (−17.0)	−18.0	−12.4, −26.0 (−19.2)	−20.2
(7)	+21.3	+19.5	152	+4.16	+13.0	+14.8	+19.5	+17.1
μ-H(5,6), (8,9)				−3.36(2)				
$P(C_2H)_3$				+3.49[e]				

[a] $\delta(^{31}P)$ at 300 K: −39.5 ppm *quartet*. Chemical shift data are given in parts per million. Comparison NMR data for $[B_9H_{13}NCS]$ $[N(PPh_3)_2]$ (**8**) and $[B_9H_{13}NCMe]$ (**9**) were taken from ref 22d. [b] DFT-GIAO//B3LYP/6-31G* calculated ^{11}B chemical shifts are given. Average shift is shown in parentheses. [c] Doublet probably due to coupling to ^{31}P with $^{3}J(^{31}P-^{1}H) = 33.2$ Hz. [d] Doublet, $^{2}J(^{31}P-^{11}B) = 104$ Hz. [e] $^{3}J(^{31}P-^{1}H) = 10.3$ Hz.

There are also inconsistencies in published perceptions about the inner-sphere open-face hydrogen-atom distribution in the family of neutral, rather than anionic, ligand species [*arachno*-B_9H_{13}-4-L]. As mentioned above in the context of the $[B_9H_{14}]^-$ configuration, an ab initio/IGLO/NMR study that compares the computed chemical shifts and the geometry of a range of *arachno*-nonaborane species was published contemporaneously with our ongoing experimental work that is the basis of this present paper.[19] The results suggested the {3×μ-H, 2×*endo*} structure **VIII** for $[B_9H_{13}(NCMe)]$ **9**, in contrast to the experimental conclusion[15b,c] by Lipscomb and co-workers that the species had the {2×μ-H, 3×*endo*} configuration **IV**. Members of the $[B_9H_{13}$-4-L] family are relatively simple to synthesize and also occur as byproducts in a variety of reactions. Since the initial structural study on $[B_9H_{13}(NCMe)]$ **9** by Lipscomb and co-workers,[15b,c] a range of them have been characterized by NMR spectroscopy.[5,22] However, possibly due to the perception that the structural class was fully described by Lipscomb's study, no further structurally defined examples of the class have been published: the one exception to this generalization is compound **8**,[20] mentioned above, which is in any event anionic and not neutral. We have therefore looked to examples of $[B_9H_{13}L]$ species that have arisen during related work in our laboratories over some time and have thereby extended the number of cases with single-crystal X-ray diffraction studies to include four additional $[B_9H_{13}L]$ species, specifically those where L = $P(CCH)_3$ (**3**), $NHEt_2$ (**4**), NC_5H_5 (**5**), and NH_2CH_2Ph (**6**). We have also extended the computational work by performing density functional theory (DFT) calculations on further representative $[B_9H_{13}L]$ species, specifically where L = $P(CCH)_3$ (**3**), $NHEt_2$ (**4**), $\{NCS\}^-$, as in compound **8**, and MeCN (**9**) (Table 5). Selected calculated and experimental interatomic dimensions for **3**−**6** are given in Table 6, and projection views of the molecular structures are shown in Figure 2.

Allowing for the inherent limited accuracy of the X-ray diffraction technique in the location of hydrogen atoms, an examination of the detailed interatomic dimensions shows a set of results that are consistent with regard to the hydrogen-atom positions in these compounds, suggesting that the data do now provide a reasonable consensus for the positions of the open-face inner-sphere hydrogen atoms in this class of compound. The {3×μ-H, 2×*endo*} configuration, together with the bridging hydrogen atom asymmetry that is evident for the $[B_9H_{12}Br_2]^-$ and $[B_9H_{14}]^-$ anions in compounds **1** and **2** is mirrored in

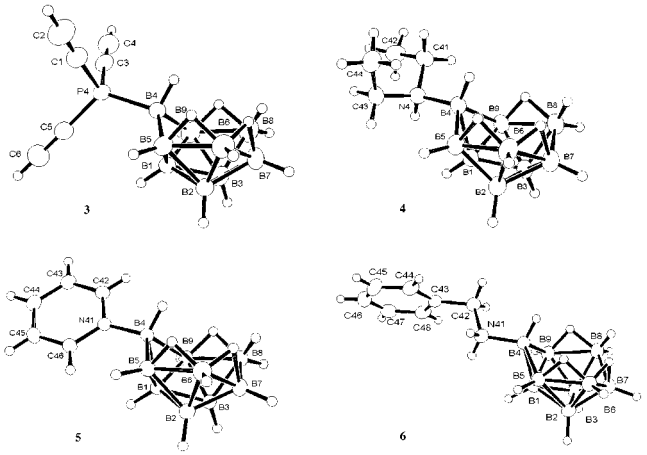

Figure 2. Crystallographically determined molecular structures, drawn with 50% probability ellipsoids and with hydrogen atoms shown as small circles of arbitrary radii, for [*arachno*-B_9H_{13}-4-$(PCCH)_3$] **3**, [*arachno*-B_9H_{13}-4-$(NHEt_2)$] **4**, [*arachno*-B_9H_{13}-4-(NC_5H_5)] **5**, and [*arachno*-B_9H_{13}-4-(NH_2CH_2Ph)] **6**.

compounds **3**−**6**. For example, the μH6,7 atoms show consistently shorter distances to the B6 positions at 1.15(2)−1.230(15) Å than to the B7 atoms at 1.352(17)−1.54(2) Å. Similarly, the μH8,9 atoms are closer to the B9 than to the B8 atoms [1.268(18)−1.282(14) versus 1.268(18)−1.348(15) Å]. The pairs of bridging hydrogen atoms attached to the B6 atoms in these ligated species feature very long B−H distances of 1.352(17)−1.54(2) Å to the B7 atom versus 1.15(2)−1.230(15) Å in the shorter arm to the B5 atom, similar to the differential distances in the $[B_9H_{14}]^-$ anion in **2** [1.32(2) versus 1.20(2) Å] and are in general agreement with the calculated values shown in Table 6. The extreme distance of 1.54(2) Å in $[B_9H_{13}NC_5H_5]$ **5** is probably partly a result of experimental uncertainty in hydrogen-atom location.

The interatomic distances for equivalent heavy-atom pairs in the series are very similar within experimental error. Similarly to the equivalent positions in the $[B_9H_{12}Br_2]^-$ and $[B_9H_{14}]^-$ anionic clusters in compounds **1** and **2**, the group of $[B_9H_{13}L]$ compounds **3**−**6** feature longer connections spanning B4−B5 and B7−B8, with the connectivities for the amine compounds **4** and **6** at ca. 1.9044(16)−1.981(2) Å being ca. 0.06−0.10 Å longer than for the phosphine compound **3** and the pyridine species **5**. These longer distances are comparable to the long "gunwale" distances of 1.973(4) Å in *nido*-decaborane(14).[50] Interestingly, the experimentally observed distances for the B4−B5/B7−B8 pair in **3** are somewhat shorter than the calculated

Table 6. Selected Calculated and Experimental Interatomic Distances and Angles for $[B_9H_{13}P(C_2H)_3]$ (**3**), $[B_9H_{13}NHEt_2]$ (**4**), $[B_9H_{13}NC_5H_5]$ (**5**), and $[B_9H_{13}NH_2(CH_2Ph)]$ (**6**)[a]

	3	4	5	6		3	4	5	6
B1−B4	1.732(2) [1.735]	1.726(2) [1.726]	1.729(2)	1.723(2)	B1−B9	1.749(2) [1.749]	1.742(2) [1.735]	1.743(2)	1.741(2)
B1−B5	1.751(2) [1.760]	1.737(1) [1.744]	1.747(2)	1.740(2)	B1−B3	1.758(2) [1.756]	1.772(1) [1.764]	1.766(2)	1.768(2)
B1−B2	1.764(2) [1.756]	1.775(1) [1.775]	1.775(2)	1.782(2)	B3−B7	1.775(2) [1.738]	1.7490(2) [1.736]	1.766(2)	1.749(2)
B3−B8	1.750(3) [1.782]	1.762(2) [1.781]	1.742(2)	1.775(2)	B3−B9	1.798(2) [1.816]	1.795(2) [1.806]	1.801(2)	1.792(2)
B2−B3	1.791(2) [1.804]	1.808(2) [1.810]	1.803(2)	1.806(2)	B2−B6	1.724(2) [1.714]	1.7210(2) [1.714]	1.734(2)	1.714(2)
B2−B7	1.777(2) [1.778]	1.767(2) [1.770]	1.771(2)	1.775(2)	B2−B5	1.797(2) [1.805]	1.798(2) [1.799]	1.796(2)	1.804(2)
B4−B5	1.843(2) [1.873]	1.904(2) [1.894]	1.858(2)	1.909(2)	B4−B9	1.843(2) [1.833]	1.858(2) [1.855]	1.877(2)	1.843(2)
B7−B8	1.885(3) [1.977]	1.950(2) [1.991]	1.892(2)	1.981(2)	B8−B9	1.868(3) [1.913]	1.876(2) [1.904]	1.865(2)	1.887(2)
B6−B7	1.824(3) [1.796]	1.819(2) [1.793]	1.846(2)	1.789(2)	B4−P/N4	1.8999(14) [1.924]	1.593(1) [1.616]	1.570(1)	1.5848(19)
B6−B5	1.839(2) [1.826]	1.830(2) [1.820]	1.838(2)	1.817(2)					
B9−H89	1.268(18) [1.289]	1.229(14) [1.283]	1.282(14)	1.272(18)	B8−H89	1.268(18) [1.359]	1.348(15) [1.374]	1.293(14)	1.339(16)
B6−H67	1.15(2) [1.280]	1.230(15) [1.283]	1.208(19)	1.224(17)	B7−H67	1.46(2) [1.396]	1.411(15) [1.393]	1.54(2)	1.352(17)
B5−H56	1.32(2) [1.331]	1.269(13) [1.323]	1.238(15)	1.248(16)	B6−H56	1.27(2) [1.322]	1.281(13) [1.335]	1.255(15)	1.259(17)
P4−C3	1.742(01) [1.752]				P4−C1	1.746(1) [1.762]			
C1−C2	1.171(2) [1.208]				C3−C4	1.176(2) [1.212]			
C5−C6	1.170(2) [1.209]				P4−C5	1.741(1) [1.750]			
N/P4−B4−B9	119.11(9)	114.50(8)	118.17(9)	116.82(12)	N/P4−B4−B1	116.34(9)	110.56(8)	112.30(9)	109.65(11)
B9−B4−B5	108.25(10)	104.97(8)	105.83(8)	105.07(10)	N/P4−B4−B5	116.92(9)	119.83(8)	117.26(9)	116.97(11)
B8−B7−B6	125.98(13)	121.94(9)	123.45(10)	121.18(12)	B4−B9−B8	113.08(12)	116.39(8)	115.61(9)	115.31(12)
B6−B5−B4	113.86(11)	116.70(8)	116.62(9)	117.74(11)	B7−B6−B5	103.70(10)	104.82(8)	103.54(9)	105.69(11)
C2−C1−P4	175.99(16)				C4−C3−P4	175.53(14)			
C5−C6−P4	178.63(16)								

[a] Interatomic distances are given in angstroms and angles in degrees, with s.u's in parentheses. Calculated values are shown in brackets.

distances, with 1.843(2) and 1.885(3) Å (obsd) versus 1.873 and 1.977 Å (calcd).

There remains the question of the hydrogen-atom placement in the borane cluster of $[B_9H_{13}(NCMe)]$ **9**, of which the structural elucidation as exhibiting the {2×μ-H, 3×*endo*} open-face inner-sphere configuration **IV** initially defined the area[15b,c] and has subsequently been assumed generally as the representative [*arachno*-B_9H_{13}-4-L] structural motif. This original structural analysis of the cluster in **9** was followed by the ambient-temperature study of the $[B_9H_{14}]^-$ anion in **7**, in which the hydrogen atom positions were not accurately located but for which the {2×μ-H, 3×*endo*} configuration **V** was concluded.[16b,c] The combination of these structural determinations has hitherto given rise to the perception that there were two different {2×μ-H, 3×*endo*} structural forms, one for the neutral [*arachno*-B_9H_{13}-4-L] species and the other for the anionic [*arachno*-$B_9H_{14}]^-$ species. However, our calculations and those of Hofmann and Schleyer[19] now indicate that the inner-sphere hydrogen-atom configuration of the MeCN compound **9** should also mirror that of the {3×μ-H, 2×*endo*} configuration **VIII** exhibited by all the other [*arachno*-B_9H_{13}-4-L] species. It also is apposite here to note that one of the class of macropolyhedral boranes, $B_{15}H_{23}$,[51] which consists of a $\{B_9H_{13}\}$ cage of geometry **II** that shares at its 4-position a pair of electrons with the basal B4−B5 bond of a *nido*-B_6H_{10} cage, also has the same {3×μ-H, 2×*endo*} configuration adopted by all the *arachno*-B_9H_{13}-4-L systems described in this paper.

In the initial diffraction analysis of **9**, the presence of the crystallographically imposed plane of symmetry along the CCNB1B4B7 plane presumably obscured the differentiation between a supposed third bridging hydrogen atom versus the third *endo*-terminal hydrogen that we see in the other [*arachno*-B_9H_{13}-4-L] species reported herein and elsewhere.[20,22d,51] X-ray diffraction has inherent problems in locating hydrogen atoms and this limitation, together with the presence of the symmetry plane, would obscure the observation of the asymmetric disposition of the inner-sphere hydrogen atoms. In addition, the *endo*-terminal and bridging hydrogen atoms that are associated with the B6B7B8 notch in the $[B_9H_{13}$-4-L] species rapidly exchange on the NMR time scale at all available temperatures. This fluxional exchange gives rise to the 2:2:2:1:1:1 pattern in the ^{11}B spectrum, which, in the absence of other evidence, would reasonably suggest the presence of two mutually equivalent bridging hydrogen atoms, which in turn would be consistent with a molecule with C_s symmetry, and thence consistent with

(51) (a) Huffman, J. D. Report 81902, Molecular Structure Center, Indiana University Department of Chemistry, 1981. Obtained from the website http://www.iumsc.indiana.edu/. (b) Rathke, J.; Schaeffer, R. *Inorg. Chem.* **1974**, *13*, 3008.

the early X-ray diffraction structural derivation.[15b,c] Indeed Lipscomb[15b] discarded the notion of two additional bridging H atoms because such would violate his topological rules and have two Hμ atoms on a boron atom bonded to four other boron atoms.[18] The presence of only three, noncontiguous, bridging H atoms does not violate his topological rules. As discussed above, the $[B_9H_{12}Br_2]^-$ anion in **1** (Table 4), and the $[B_9H_{13}(NCS)]^-$ anion in **8**[20,22d] also feature the {3×μ-H, 2×*endo*} configuration. In both these cases the rapid hydrogen-atom exchange is quenched at lower temperatures, revealing the presence of three B−μH−B proton NMR resonances, two being very similar in chemical shift, giving an apparent relative intensity pattern of 2:1 for the three resonances. The crystallographic plane of symmetry imposed in the crystal-structure analysis of the borane cage in compound **9** is primarily based on the location of the electron density of the non-hydrogen atoms. In this regard it may be noted that, in the original analysis of **9**, the MeCN ligand lies on the B1B4B7 symmetry plane, whereas compounds **3**−**6** contain asymmetrically orientated non-hydrogen atoms in their attached ligands, thus giving rise to space groups of lower symmetry. One consequence of this is that the two inner-sphere hydrogen atoms associated with the B6B7B8 notch would refine identically. We thence surmised that if the X-ray data for $[B_9H_{13}NCMe]$ **9** were refined in a space group of lower symmetry, then, in conjunction with the other physical and calculational evidence described above, it would provide a reasonable test for the asymmetric disposition of the hydrogen atoms in this compound. To test this hypothesis, we collected a new good-quality, low-temperature X-ray diffraction data set on a single crystal of **9** (presented as Supporting Information) and refined the structure in the appropriate space group of lower symmetry, i.e., $P2_1$ instead of $P2_1/m$. Refinement of the data in the centrosymmetric space group $P2_1/m$ thence reproduced the {3×μ-H, 2×*endo*} structural result reported by Lipscomb. However, alternative refinement in the lower-symmetry noncentrosymmetric space group $P2_1$ now clearly revealed the presence of the third bridging hydrogen atom and the adjacent *endo*-terminal hydrogen atom in the {3×μ-H, 2×*endo*} configuration **VIII** (Figure 3). The Lipscomb structure **IV**, which was refined in the ostensibly correct space group, is therefore not an exception but an artifact of the imposed symmetry plane: the imposition of the crystallographic plane of symmetry necessarily inhibited the observation of the asymmetric disposition of the inner-sphere hydrogen atoms.

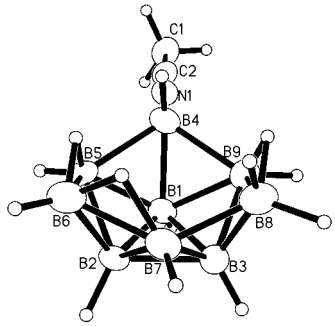

9

Figure 3. Crystallographically determined molecular structure of [*arachno*-B_9H_{13}-4-(NCMe)] **9**, from data refined in the $P2_1$ space group. This clearly shows the presence of a third bridging hydrogen atom spanning B6−B7, and an *endo*-terminal inner-sphere hydrogen atom on B8, rather than two identical *endo*-type hydrogen atoms, or two identical hybrid *endo*-bridging hydrogen atoms, at B6 and B8. Drawn with 40% probability ellipsoids and with hydrogen atoms shown as small circles of arbitrary radii.

Summary and Conclusions

We have investigated the structures of a series of *arachno*-nonaboranes, both experimentally and with theoretical calculations. These include established species as well as the new $[B_9H_{12}Br_2]^-$ anion and some new [*arachno*-B_9H_{13}-4-L] systems. We conclude that, contrary to some hitherto accepted literature reports, they all are isostructural with respect to the arrangement of the bridging and *endo*-hydrogen atoms around their cluster open faces. All have the same {2×μ-H, 3×*endo*} configuration of their open-face inner-sphere hydrogen atoms. Our experimental work adds credence to the similar conclusions arising from calculations by Hofmann and Schleyer.[19] In sum, we have provided experimental evidence supported by both MO and DFT calculations that the solid-state geometries with respect to hydrogen atom positions are the same for both the $[B_9H_{14}]^-$ and $[B_9H_{12}Br_2]^-$ anionic species and for the series of neutral and anionic [B_9H_{13}-4-L] species. Definitive statements in the literature that the important [*arachno*-B_9H_{14}]$^-$ anion is of the {2×μ-H, 3×*endo*} configuration **V** should therefore be revised in favor of the {3×μ-H, 2×*endo*} configuration **VII**, and analogous assumptions of the {2×μ-H, 3×*endo*} structures **IV** for the very well-used [*arachno*-B_9H_{13}-4-L] neutral species should also similarly be revised in favor of the {3×μ-H, 2×*endo*} configuration as in **VIII**.

Acknowledgment. We thank the EPSRC (U.K.) (Grants H97024, K05818, and L49505 and a studentship to M.G.S.L.) and the CLRC (U.K.) for support, and Simon Barrett for assistance with NMR spectroscopy. We also acknowledge the NSF (Grant CHE-9311557) and the Missouri Research Board and instrumentation grants (Grant CHE-9318696), the DOE (Grant DE-FG02-92CH10499), and the UM−St. Louis Center for Molecular Electronics, which allowed purchase of the Varian Unity Plus NMR spectrometer and the latter two along with the NSF (Grant CHE-9309690) for funds to purchase one of the X-ray diffractometers used in this work.

Supporting Information Available: Crystal data and structure refinement parameters, tables of atomic coordinates, anisotropic thermal parameters, atomic coordinates, bond lengths, and bond angles in CIF file format for **1**−**6** and **9**, and geometries in Cartesian coordinates produced from B3LYP/6-31G* optimizations for **3**, **4**, **8**, and **9** in PDF format. This material is available free of charge via the Internet at http://pubs.acs.org

JA025700D